(2)

AD-A275 079

InTlSb ANNUAL REPORT - 1993

InTlSb For Long-Wavelength Infrared Photodetectors and Arrays

ONR Contract No. N00014-92-J-1951
ONR Contract No. N00014-93-1-0409
ARPA/ONR Contract No. N00014-93-1-0931

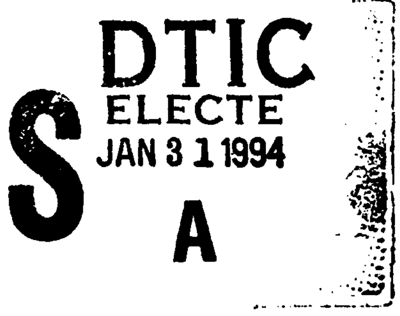

Principal Investigator
Manijeh Razeghi

Center for Quantum Devices
Dept. of Electrical Engineering and Computer Science
Northwestern University
Evanston, Illinois 60208

This document has been approved for public release and sale; its distribution is unlimited.

STAFF: Prof. E. Bigan, Prof. D. Garbouzov, Prof. L. Wang, Dr. E. Kolev, Jeff Gwilliam

STUDENTS: Yeun Choi, Guillaume Labeyrie, Cengiz Besikci, Erick Michel, Erik Quanstrom

94-02068

94 1 24 081

INTRODUCTION

The objective of this research program is to grow InTlSb alloys by low-pressure metalorganic chemical vapor deposition and to investigate their physical properties, in order to demonstrate the feasibility of long-wavelength infrared detectors based on these materials.

Ab initio theoretical calculations indicate that InTlSb is a potential alternative to HgCdTe, with the added metallurgical and processing advantages offered by III-V technology. TlSb has been predicted to be a semimetal with a bandgap of -1.5eV. Therefore, it should be possible to cover the whole infrared spectrum by alloying InSb with TlSb. In addition, TlSb is expected to remain lattice-matched to InSb within 2%, which is an advantage for the growth of device-quality InTlSb alloys. Even though TlSb was expected to favor the CsCl-type structure, InTlSb alloy was estimated to exhibit a stable zinc-blende structure up to 15-20% Tl [1,2].

Below we indicate the major achievements that have been accomplished over the last year. These are described in detail in following sections. Our plan for the coming year will be given in the final section.

HIGHLIGHTS OF THE PAST YEAR

1. Grown one of the best (structural and electrical quality) InSb on GaAs substrate. The optimization of the InSb growth conditions is now completed.

2. Demonstrated the first growth of InTlSb. Evidenced the incorporation of thallium by Auger Electron spectroscopy. Observed a shift in the absorption edge by infrared transmission and photoresponse.

3. Varied the thallium content and observed the resulting changes in physical properties.

4. Achieved D^* of 1×10^9 $cmHz^{1/2}W^{-1}$ at 7μm wavelength and 77K for a photoconductor having a 9μm cut-off wavelength. These results are better than those reported for similar InAsSb photoconductors.

DTIC QUALITY INSPECTED 5

5. Doped n- and p-type InSb grown on GaAs.

Availability Codes
Dist | Avail and / or Special
A-1

1. Growth of high-quality InSb

Growth

Trimethylindium (TMI) and trimethylantimony (TMSb) were used as precursors. Their respective bubbler temperature were kept at 18°C and 0°C. The growths were carried out on InSb, semi-insulating GaAs, and GaAs coated Si substrate. The latter was investigated because of the possibility for future integration of infrared detection and signal processing circuits on the same substrate. Superclean GaAs and GaAs/Si substrates were directly loaded into the growth chamber without any preparation. During the heating of the substrate, a pregrowth arsine overpressure was maintained in order to prevent any surface degradation. For InSb substrates, the best preparation method was found to be etching in lactic acid:nitric acid (10:1) mixture. However, we observed that this etching reveals line defects on some InSb substrates. The line defects are believed to originate from the lapping-polishing stages of the substrate preparation.

The optimum InSb growth conditions were found by varying the growth temperature and V/III ratio. Based upon the surface morphology of InSb films, V/III ratio of 10 was found to be optimum at a growth temperature of 465 °C [3]. Further decrease in V/III ratio degraded the morphology, and indium droplets formed on the surface; the latter phenomenon was confirmed by dissolution of these droplets in hydrochloric acid, which preferentially etches indium [4].

Characterization

Under the optimum conditions, mirror-like InSb epilayers were grown on all substrates. The film grown on InSb had x-ray FWHM of 14 arcsec while films grown on GaAs and GaAs/Si exhibited a FWHM of 171 and 361 arcsec, respectively. This trend is consistent with an increase in dislocation density with lattice mismatch. These FWHM values are among the best reported for InSb films of comparable thickness on the respective substrates, independently of the growth technology.

X-ray diffraction measurements were also performed on InSb films grown on GaAs substrate with film thickness varying from 0.95μm to 4.85μm, and the x-ray FWHM was found to decrease with increasing film thickness. This is consistent with similar observations by other authors[5,6]

The electrical properties of the epilayers were investigated through Hall measurements using the Van der Pauw method on clover-shaped samples. The ohmic contacts are made on the samples by alloying with In-Sn at 350°C under 10% H_2:90%N_2 ambient. The current and magnetic field directions are separately reversed to eliminate any Hall-probe misalignment.

The room temperature Hall mobility also reflected the improvement of the InSb/GaAs epilayer quality with increasing thickness. These trends again reflect the decrease of dislocation density away from the interface. A 4.85μm-thick InSb film exhibited room temperature Hall mobility as high as (6-7)x10^4 cm^2/Vs, which is a state-of-the-art result for films of similar thicknesses. The Hall coefficient R_H was negative and the carrier concentration of the InSb films was generally in the range of 1x10^{16} cm^{-3} to 3x$10^{16}$$cm^{-3}$ at 300K, which is close to the intrinsic carrier concentration.

As a mean of determining the effect of dislocation on the electrical properties, Hall effect measurements were performed at low temperatures where lattice scattering is reduced and impurity and defect scattering is enhanced. InSb/GaAs samples of different thicknesses were used and the temperature was varied from room temperature down to 4K. The measured Hall data displayed a behavior that could not be explained just by the combined effects of various scattering mechanisms; the Hall coefficient remained negative over entire temperature range (indicating n-type), but the Hall mobility decreased dramatically far below expected values for n-type InSb. In order to explain this behavior, the Hall mobility and Hall coefficient have been simulated using a three layer model including a surface electron accumulation layer, an interface layer with high density of dislocations, and a bulk like layer with a highly reduced defect density [7]. This theoretical analysis has shown that the InSb films are p-type and the behavior is attributed to donor-like dislocations caused by the large mismatch and to a surface layer which dominates the transport in the material at low temperatures. The results of this model provides good agreement with the experimental observations as well as with other studies reporting the growth of p-type InSb on GaAs substrates [8,9].

In spite of these results, independent studies on these InSb samples transport properties have suggested it might be n-type [10]. This study was based on magnetic field dependence of Hall mobility and magnetoresistance. The magnitude of the observed changes as a function of magnetic field strength was too large to be explained using a conventional two carrier model. By considering the material to be n-type and the existence of a surface conduction layer, the calculated results were consistent with the measured

values. These investigations suggest a complex electrical conduction scheme in InSb that needs to be addressed further not only to get a better understand of InSb electrical properties but also to help analyze the electrical properties of its alloys.

2. Demonstration of the first growth of InTlSb

Cyclopentadienylthallium (CPTl) was used as the source of thallium. CPTl is a solid with low vapor pressure at room temperature and sublimes at 120°C in vacuum (~0.1 torr). It has been previously used for growing thallium(III) oxide, a compound that has drawn interest with the discovery of high-temperature superconducting Tl-Ba-Ca-Cu oxide [11]. Thallium flow was introduced into the growth chamber without perturbing other growth parameter settings.

This has lead to the first successful growth of InTlSb [12]. The InTlSb layer was grown on top of an InSb buffer layer. The thallium incorporation was confirmed through several independent measurements: x-ray diffraction, Auger electron spectroscopy, and optical measurements. The x-ray profile taken at (800) diffraction orientation showed resolved peaks corresponding to InSb and InTlSb. As compared to a InSb reference Auger spectrum, the spectrum of InTlSb exhibited an additional peak associated to thallium [13]. However, the absolute composition of the alloy could not be determined since a InTlSb with known Tl concentration is not available for calibration purpose. Lastly, infrared transmission measurement, performed using a Fourier Transform Infrared spectrometer (FTIR), indicated a clear shift in the absorption edge as compared to that of InSb.

A more accurate assessment of the absorption edge was determined by photoconductivity measurement. As our photoconductor, the same clover-shaped sample employed in Hall measurements was used. The active area was measured to be about 4.4mm^2 with 3mm electrode spacing. The photoconductor spectral response was obtained by comparing the photoconductor under test to the spectrometer internal pyroelectric detector, and by correcting for the slow frequency response of the pyroelectric detector. This correction is necessary since the photoconductor photodetectors such as the ones to be characterized exhibit a flat frequency response but exhibit strong spectral variations as opposed to a flat spectral response and slow speed of response of the internal pyroelectric detector. The photoresponse of the InTlSb sample extended up to 8μm at 77K.

3. Growth of InTlSb alloys having various Tl content

Following this successful growth of InTlSb, the thallium content was varied in order to further extend the optical cutoff wavelength of the alloy [14]. This was achieved by varying the thallium flow and bubbler temperature, as summarized in table 1. In this study, a nominal structure was adopted: it consisted of a 1 hour growth of InSb buffer layer followed by a 1 hour growth of InTlSb. All the layers were nominally undoped. A few samples having thicker InTlSb epilayers were grown in order to improve the external quantum efficiency of the photoconductors.

Growth temperature	465 °C
Growth pressure	76 Torr
TMI flow rate	50 cc/min
TMSb flow rate	20 cc/min
CPTl flow rate	3 - 20 cc/min
CPTl bubbler temperature	0 - 80 °C

Table 1 - Growth conditions for InTlSb

Morphology was poorer than our best InSb results, and similar to that of our first InTlSb sample. However, the x-ray spectra at (800) orientation for all the samples revealed two distinct peaks that were far more resolved than our first reported result. A typical x-ray profile is given in figure 1. As mentioned previously, one of the peak is attributed to the InSb buffer layer and the other one to the InTlSb epilayer. This assertion is supported by the fact that the InSb peak remains at the same angular position while the InTlSb peak broadens and shifts away from the InSb peak as the thallium content is increased. The broadening of the InTlSb peak is believed to be a result of the increase in dislocation density as mismatch with respect to InSb increases. This hypothesis is supported by figure 2 which plots the InTlSb x-ray FWHM as a function of lattice-mismatch between InTlSb and InSb (determined from the x-ray profile). Surprisingly, a lattice contraction is observed with increasing thallium content instead of the predicted dilation [1,2].

As expected, we observed a shift of the optical absorption edge of the material towards longer wavelengths as the thallium content was increased, thus confirming a decrease of its bandgap. Figure 3 shows a set of normalized photoresponse spectra of various InTlSb and

figure 4 shows the quasi-linear observed relationship between the lattice mismatch and the cutoff wavelength (determined as the wavelength for which photoresponse falls at 10% of its maximum value). This suggests that the photoresponse cutoff wavelength can be increased further by increasing thallium content. This is in marked contrast with InAsSb which exhibits a minimum bandgap as a function of As content. Furthermore, a 9μm cutoff wavelength corresponds to a lattice mismatch of -1.3%, which is about 4 times smaller than that for InAsSb alloy having a similar cutoff wavelength. This is important for the development of device-quality material with reduced dislocation.

A rough estimate of the alloy stoichiometry can be obtained assuming a low temperature bandgap of -1.5 eV for TlSb and a linear dependence of the bandgap on thallium content [1,2]. A cutoff wavelength shift from 5.5μm for InSb up to 9μm for $In_{1-x}Tl_xSb$ corresponds to an approximate 88meV bandgap reduction and to an estimated x=0.06 thallium content. However, it should be noted that the theoretical lattice mismatch corresponding to InTlSb of this composition (obtained from Vegard's law) deviates significantly from the experimental results. This demonstrate the inconsistency in the theoretical predictions. Thus the theoretical parameters should be used with caution.

A number of trends have been observed in the electrical properties of InTlSb. Hall measurements indicated a room temperature Hall mobility ranging from 50,000 cm^2/Vs to 20,000 cm/Vs, and an electron concentration ranging from $1x10^{16}$ cm^{-3} to $5x10^{16}$ cm^{-3} for the nominal InTlSb samples, as shown in figure 5. The Hall mobility decreased monotonically with increasing thallium flow, while the electron concentration simultaneously increased. The increase in electron concentration is typical of an intrinsic semiconductor with decreasing bandgap. The decrease in mobility is attributed to an increase in alloy scattering. Measurements at 77K indicate an opposite trend for the mobility and scattered data for the electron concentration (figure 6). This behavior is likely to occur because of the dominant contribution of parallel conduction layers at low temperature, as evidenced in InSb epilayers through temperature-dependent Hall measurements.

4. InTlSb photoconductor detectivity

Detectivity estimation

The photoconductor responsivity spectrum was recorded at various bias voltages using a circuit board that acts as both a dc-current source and an ac-preamplifier delivering an output signal compatible with the Fourier Transform input of the spectrometer. Such circuit board is the standard that is used in FTIR spectrometers equipped with HgCdTe photoconductors. When the bias is varied, the overall shape of the photoresponse spectrum does not change, but its magnitude changes.

The responsivity $\Re$ of a photoconductor is expressed by

$$\Re = \eta \frac{e}{h\nu} G \tag{1}$$

where η is the absorption quantum efficiency, e the electron charge, $h\nu$ is the incident photon energy and G is the photoconductive gain. At low bias, the responsivity increases linearly with bias, because the photoconductive gain is a linear function of the bias as shown by the following relation

$$G = \frac{\mu\tau V_a}{d^2} \tag{2}$$

where $\mu\tau$ is the carrier mobility-lifetime product, V_a is the applied bias voltage, and d is the spacing between the contacts. At higher bias, the responsivity saturates and eventually decreases because of sample heating.

Neglecting Fabry-Perot oscillations for a first approximation, the quantum efficiency η is expressed as:

$$\eta = (1 - R)(1 - e^{-\alpha L}) \tag{3}$$

where R is the reflection coefficient at the front surface, α is the absorption coefficient, and L is the epilayer thickness. The reflection coefficient R can be calculated through

$$R = \frac{(n-1)^2}{(n+1)^2} \tag{4}$$

where n is the refractive index of the epilayer. In the case of InTlSb, n≈4 which implies R≈0.36, assuming the refractive index of InTlSb is comparable to that of InSb. The absorption coefficient α values are collected from transmission measurements. Combining these values, the quantum efficiency can be estimated using equation 3.

From the slopes of the linear sections of the responsivity versus bias data and from the calculated quantum efficiencies, the gain per applied bias voltage (G/V_a) can be determined. With this information, the noise current i_N can be calculated. The two contributions to the detector noise are generation-recombination noise and Johnson noise [15], so the total noise current is expressed by:

$$i_N = \sqrt{4eGi\Delta f + \frac{4kT}{r_d}\Delta f} \qquad (5)$$

where Δf is the frequency interval over which the noise is measured, r_d is the photoconductor resistance, i is the average current flowing through the photoconductor ($i=V_a/r_d$), and kT is the thermal energy. The specific detectivity D^* is then given by:

$$D^* = \frac{\Re}{i_N}\sqrt{A}\sqrt{\Delta f} \qquad (6)$$

where A is the photoconductor area.

Performance of InTlSb photoconductors

As the thallium flow was varied, the specific detectivity D^* at 7μm increased from 10^8 $cmHz^{1/2}W^{-1}$ up to $3x10^8$ $cmHz^{1/2}W^{-1}$ [14,16]. This results mainly from the increase in quantum efficiency. This quantum efficiency is improved in the case of the thick InSb/InTlSb/InSb sample grown under the condition that yielded a 9μm cutoff wavelength. X-ray diffraction pattern and photoresponse spectrum were quite similar to those of the thin structure, thus indicating good composition control. The room temperature Hall mobility increased from $2x10^4$ cm^2/Vs for the thin structure to $3x10^4$ cm^2/Vs for the thicker one. This improvement in material quality was confirmed by an increase in the photoconductive gain over bias ratio G/V. The thicker sample presents both a higher absorption quantum efficiency and a higher photoconductive gain which results in a significantly larger specific detectivity $D^*=1x10^9$ $cmHz^{1/2}W^{-1}$ at $\lambda=7\mu m$.

5. n- and p-type doping of InSb

Doping of InSb is a required step towards realization of photovoltaic detectors. Si has been previously used as a n-type dopant in the growth of InSb by MBE [17]. In our investigation, silane (SiH_4) has been tentatively tried as the Si source. However, no significant doping levels were obtained, which was attributed to low pyrolysis efficiency of silane at our growth temperature [18]. To determine the validity of this assertion, di-silane (Si_2H_6) has been investigated because it is known to pyrolyze completely at this temperature. The flow ranged from 50cc/min to 1500cc/min. Once again, the measurements showed no conclusive evidence of a doping trend.

Tetraethyltin (TESn) has been used as an alternative n-type dopant source. The flow was varied from 7cc/min to 80cc/min, resulting in doping levels ranging from $5\times10^{16}cm^{-3}$ to $1.2\times10^{18}cm^{-3}$ (figure 7). No degradations in surface morphology and x-ray FWHM were observed. Furthermore, we did not notice any memory effect associated with the use of TESn. These results are consistent with other reported work [19].

From the literature, there seems to be fewer satisfactory choices among the available p-type dopant sources. One of those, dimethylzinc (DMZn), was used with its bubbler held at a constant temperature at -25°C. The flow rates, which varied from 2 cc/min and 10cc/min, were diluted after passing through the bubbler. Dilution flow was kept at 1200 cc/min. The lowest concentration of 3.0×10^{18} cm^{-3} was obtained with a flow of 2 cc/min. Diethylzinc (DEZn) was also reported to result in similar doping concentrations [20].

CONCLUSION

Reproducible growth of high quality InSb films have been mastered. InSb films were grown on InSb, GaAs, and Si substrates and characterized using Nomarski interference microscope, high resolution x-ray diffraction, and Hall measurements. The results of these characterizations have proven the structural and electrical quality of the films to be among the best reported so far.

Once this preliminary step was achieved, the first successful growth of InTlSb was demonstrated. Several independent characterization methods evidenced the formation of the ternary compound InTlSb, with a bandgap smaller than that of InSb and a reduced lattice parameter.

The next phase of this program was the study of the InTlSb alloy bandgap tailoring, by means of varying its composition. This work so far resulted in the growth of various alloys, with maximum photoresponse cutoff wavelength up to 9μm. There is no experimental indication that the cutoff wavelength cannot be extended further. Under the growth conditions yielding a cutoff wavelength of 9μm, a thick sample was grown which resulted in a photoconductor with a specific detectivity of $D^*=10^9$ $cmHz^{1/2}W^{-1}$ at $\lambda=7\mu m$. This result is better than those reported for similar InAsSb photoconductors [21].

In parallel, doping of InSb is being carried out as an initial step towards the realization of photovoltaic detectors. Reproducible n-type doping concentrations from 5×10^{16} cm^{-3} to 1.2×10^{18} cm^{-3} have been obtained using tetraethyltin. P-type doping was achieved using dimethylzinc in the range of 3.0×10^{18} cm^{-3} to 3×10^{19} cm^{-3}. Both dopant sources had no degradation effects on the InSb epilayer quality.

FUTURE WORK

Further characterization of epitaxial layers

Our knowledge of the physical properties of InTlSb is insufficient at present. Even though we have demonstrated a reduction in the bandgap with increasing thallium content, the sign and magnitude of the lattice mismatch does not agree with theoretical calculations. In a recent letter, Arden Sher suggested that our material might be inhomogeneous, with possible TlSb inclusions. We plan to further investigate the structural properties of InTlSb epilayers by using X-ray micrography and transmission electron microscopy. This should determine whether the material is homogeneous or not.

We also plan to investigate the uniformity of the InTlSb epilayers by repeating our photoresponse measurements with focusing the infrared beam (so far, our photoresponse measurements have been performed with the infrared beam overfilling a photoconductor with approximate area $4mm^2$, so that it does not provide any information about the uniformity). We plan to further investigate the optical properties of InTlSb using infrared photoluminescence. For this purpose we will upgrade an existing luminescence set-up operating in the visible to near-infrared. Photoluminescence will be useful to compare epilayers grown on InSb and GaAs substrate. Besides, we will use photoluminescence to assess the epitaxial layer uniformity.

Growth of InTlSb by low-pressure MOCVD

We need to expand the significant achievements of last year (first growth of InTlSb, variation of the thallium content). Effort will be put towards optimizing the growth conditions of InTlSb in order to improve the morphology and the crystalline quality. The X-ray full-width-at-half-maximum of InTlSb epilayers has been considerably improved between the first successful growth of InTlSb and the present results, and there is no reason to believe that these current results constitute any fundamental limitation.

We need to increase the thallium content so as to extend the cut-off wavelength up to 12μm. Various approaches have to be attempted in order to increase the thallium content while maintaining a reasonable crystal quality. The reduction of the growth temperature is one of them. We need to check whether there is any correlation between the epilayer homogeneity and the thallium content.

In order to confirm the full potential of InTlSb for infrared detection, we need to demonstrate photovoltaic detectors based on p-n junctions as well. The doping study of InSb being now almost completed, we will start doping InTlSb and grow p-n structures for photovoltaic detection.

Growth of InTlSb by molecular beam epitaxy

The delivery of the MBE reactor dedicated to InTlSb is scheduled this month (January 1994). Once operational, we will determine the optimum growth conditions of InSb on both GaAs and InSb substrates, and will shift rapidly to the growth of InTlSb. There are several advantages in using MBE for the growth of InTlSb. First, MBE is well suited for the growth of uniform layers on two-inch wafers which is essential for the development of focal-plane arrays. The transfer to industry of the developed know-how might also prove easier with MBE. Second, MBE has a number of in-situ characterization techniques (such as RHEED) that will be most helpful in optimizing the growth conditions and understanding the physical properties of the epilayers. Third, we will rule out any artifact linked to the growth process by comparing the results obtained by LP-MOCVD and MBE. By comparing MOCVD with MBE results, we will be able to ascertain the physical properties of InTlSb.

Fabrication and characterization of infrared detectors

We need to establish simple methods for the fabrication and characterization of photodiodes in order to provide a rapid feedback to the growth process, similar to the methods we use for photoconductivity. On the basis of previous work on conventional InSb photodetectors, we need to develop fabrication and characterization methods for optimized photodetectors compatible with focal-plane arrays. Mesa etching, metallization, junction passivation, anti-reflection coating, and appropriate mounting are some of the steps that need to be established in order to convince the industrial community of the interest of InTlSb alloys. We also need to improve our characterization methods. In particular, we need to perform accurate noise measurements, to improve our D^* estimates.

REFERENCE

1. M. van Schilfgaarde, A. Sher, and A.-B. Chen, Appl. Phys. Lett. 62, 1857, (1993).

2. A.-B. Chen, M. van Schilfgaarde, and A. Sher, J. of Electron. Mater. 22, 843, (1993).

3. Y.H. Choi, R. Sudharsanan, C. Besikci, E. Bigan, and M. Razeghi, Mat. Res. Soc. Symp. Proc. 281, 375, (1993).

4. R.M. Biefeld, J. Crystal Growth 75, 255, (1986).

5. R.M. Biefeld and G.A. Hebner, J. Crystal Growth 109, 272, (1991).

6. C.F. McConville, C.R. Whitehouse, G.M. Williams, A.G. Cullis, T. Ashley, M.S. Skolnick, G.T. Brown, and S.J. Courtney, J. Crystal Growth 95, 228, (1989).

7. C. Besikci, Y.H. Choi, R. Sudharsanan, and M. Razeghi, J. Appl. Phys. 73, 5009, (1993).

8. J.R. Soderstrom, M.M. Cumming, J-Y. Yao, and T.G. Andersson, Semicond. Sci. Technol. 7, 337, (1992).

9. G.M. Williams, C.R. Whitehouse, C.F. McConville, A.G. Cullis, T. Ashley, S.J. Courtney, and C.T. Elliot, Appl. Phys. Lett. 53, 1189, (1988).

10. S.N. Song, J.B. Ketterson, Y.H. Choi, R. Sudharsanan, and M. Razeghi, Appl. Phys. Lett. 63, 964, (1993).

11. A.D. Berry, R.T. Holm, R.L. Mowery, N.H. Turner, and M. Fatemi, Chem. Mater. 3, 72, (1991).

12. Y.H. Choi, C. Besikci, R. Sudharsanan, and M. Razeghi, Appl. Phys. Lett. 63, 361, (1993).

13. Y.H. Choi, P.T. Staveteig, E. Bigan, and M. Razeghi, J. Appl. Phys. 75, (1994).

14. E. Bigan, Y.H. Choi, G. Labeyrie, and M. Razeghi, Proceedings of SPIE, Los Angeles, California, (1994).

15. A. Rose, "Concepts in photoconductviity and allied problems", Wiley, New York, (1963).

16. P.T. Staveteig, Y.H. Choi, G. Labeyrie, E. Bigan, and M. Razeghi, to be published in Appl. Phys. Lett., (1994).

17. R.A. Stradling, Semicond. Sci. Technol. 6, C52, (1991).

18. G.B. Stringfellow, "Organometallic Vapor-Phase Epitaxy: Theory and Practice," Academic Press, (1989).19. R.M. Biefeld, S.R. Kurtz, and I.J. Fritz, J. of Electron. Mat. 18,775, (1989).

19. R.M. Biefeld, J.R. Wendt, and S.R. Kurtz, J. of Crystal Growth 107, 836, (1991).

20. R.M. Biefeld, S.R. Kurtz, and I.J. Fritz, J. of Electron. Mat. 18,775, (1989).

21. C.G. Bethea, B.F. Levine, M.Y. Yen, and A.Y. Cho, Appl. Phys. Lett. 53, 291, (1988).

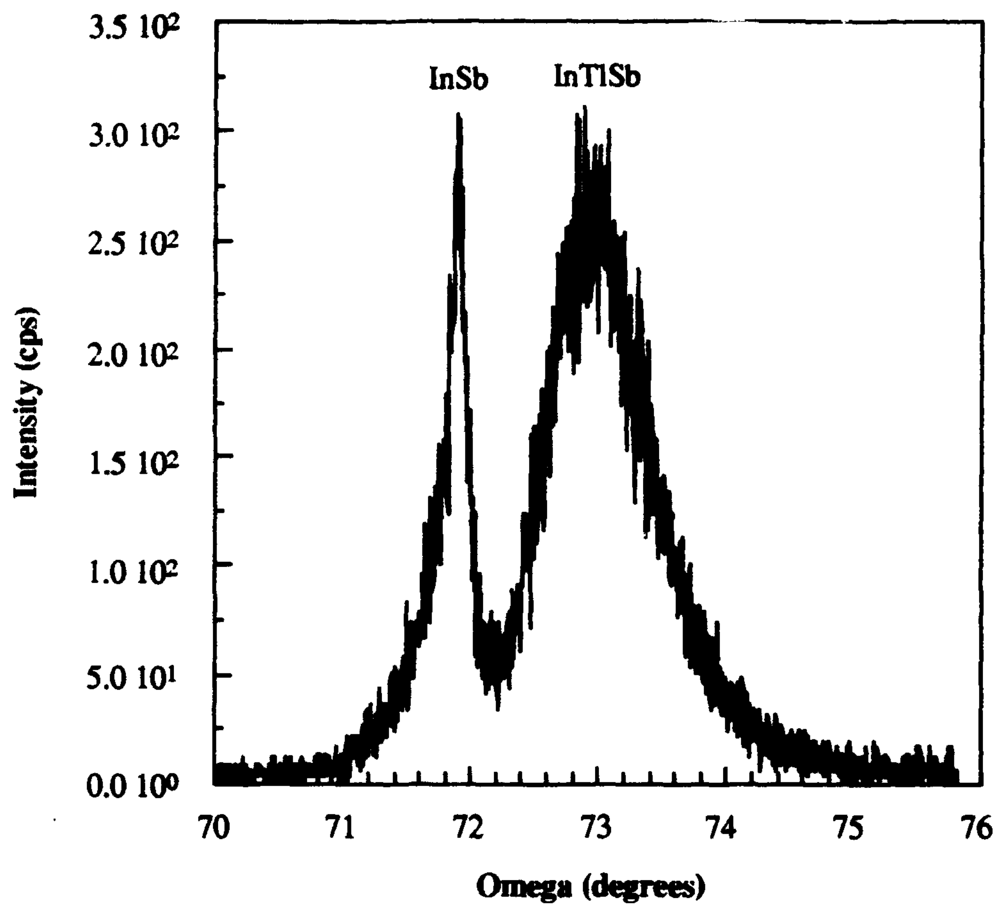

Figure 1 X-ray diffraction rocking curve of an InTlSb sample. This was measured at (800) diffraction orientation. In addition to the InSb buffer layer peak, a peak corresponding to InTlSb is resolved.

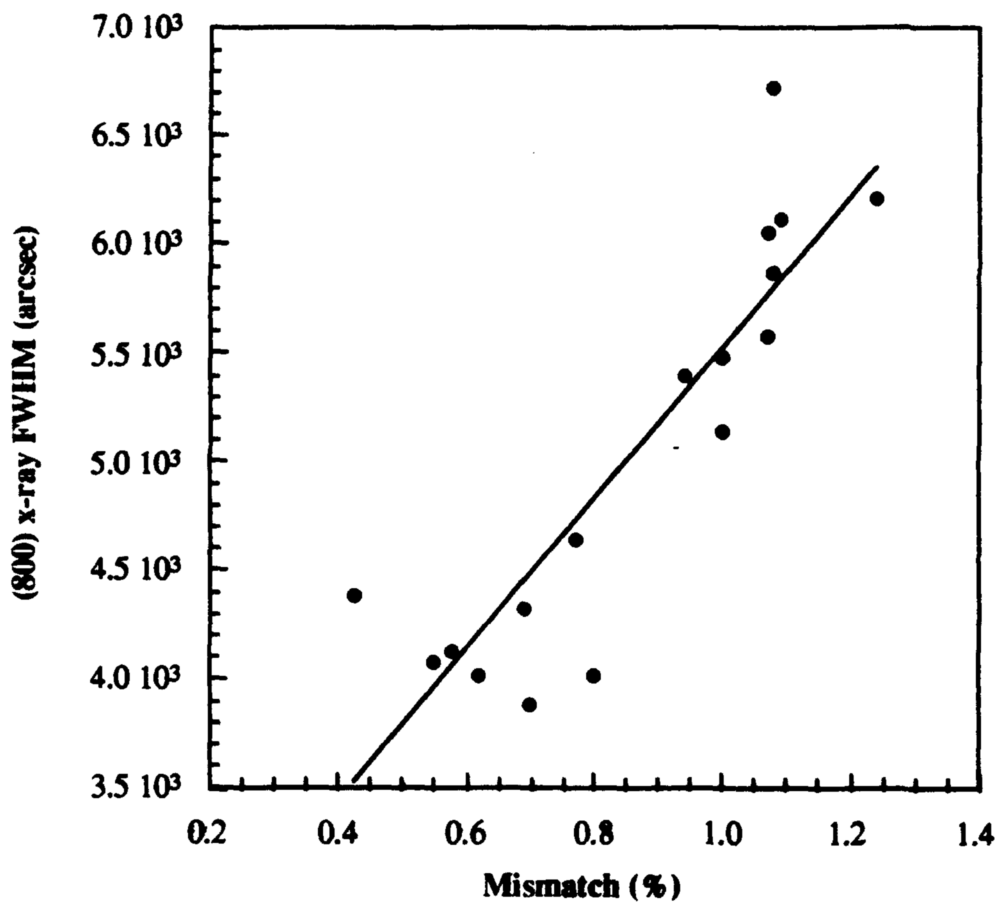

Figure 2 Relationship between InTlSb x-ray FWHM and its lattice mismatch with InSb.

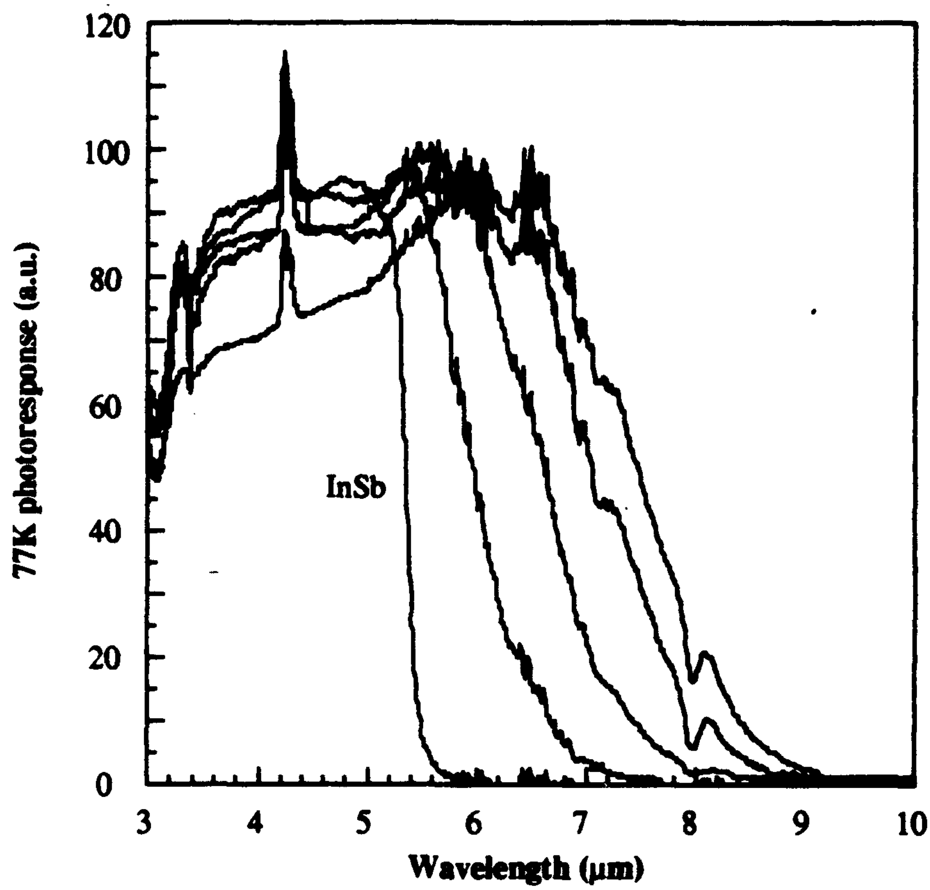

Figure 3 Normalized photoconductor spectral response of various InTlSb alloys at 77K

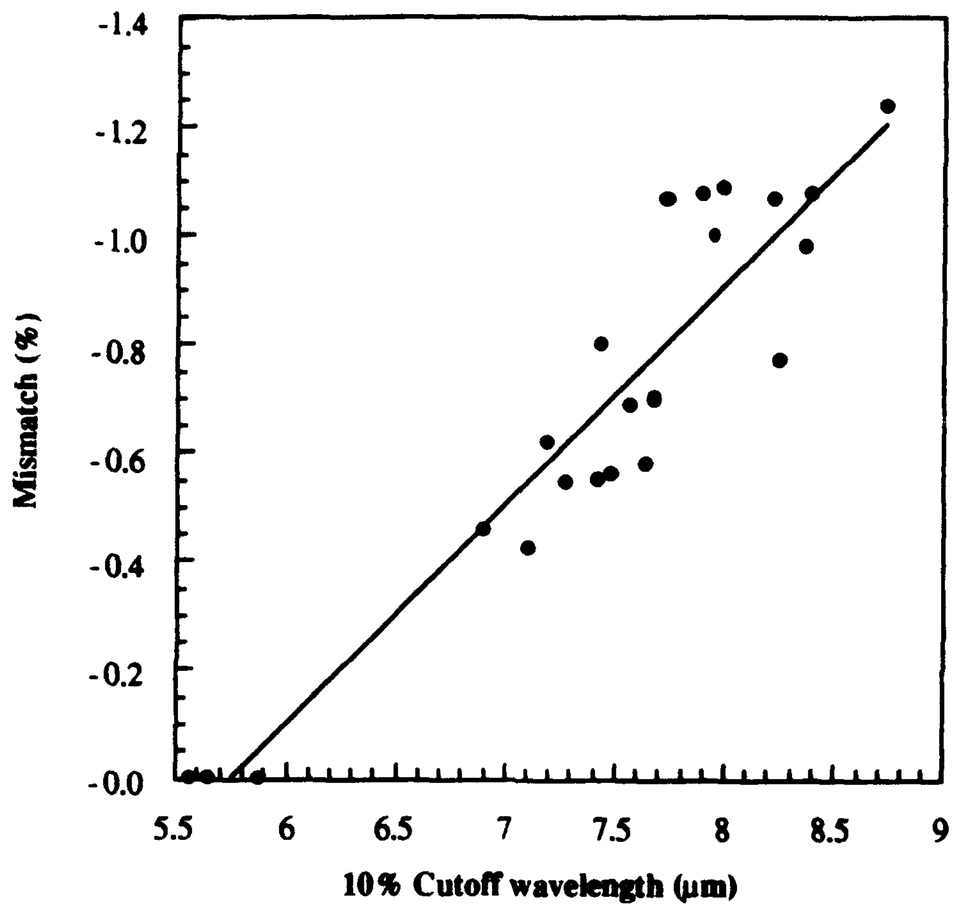

Figure 4 Lattice mismatch between InTlSb and InSb versus 77K photoresponse cutoff wavelength (defined as the wavelength for which the photoresponse falls at 10% of its maximum value).

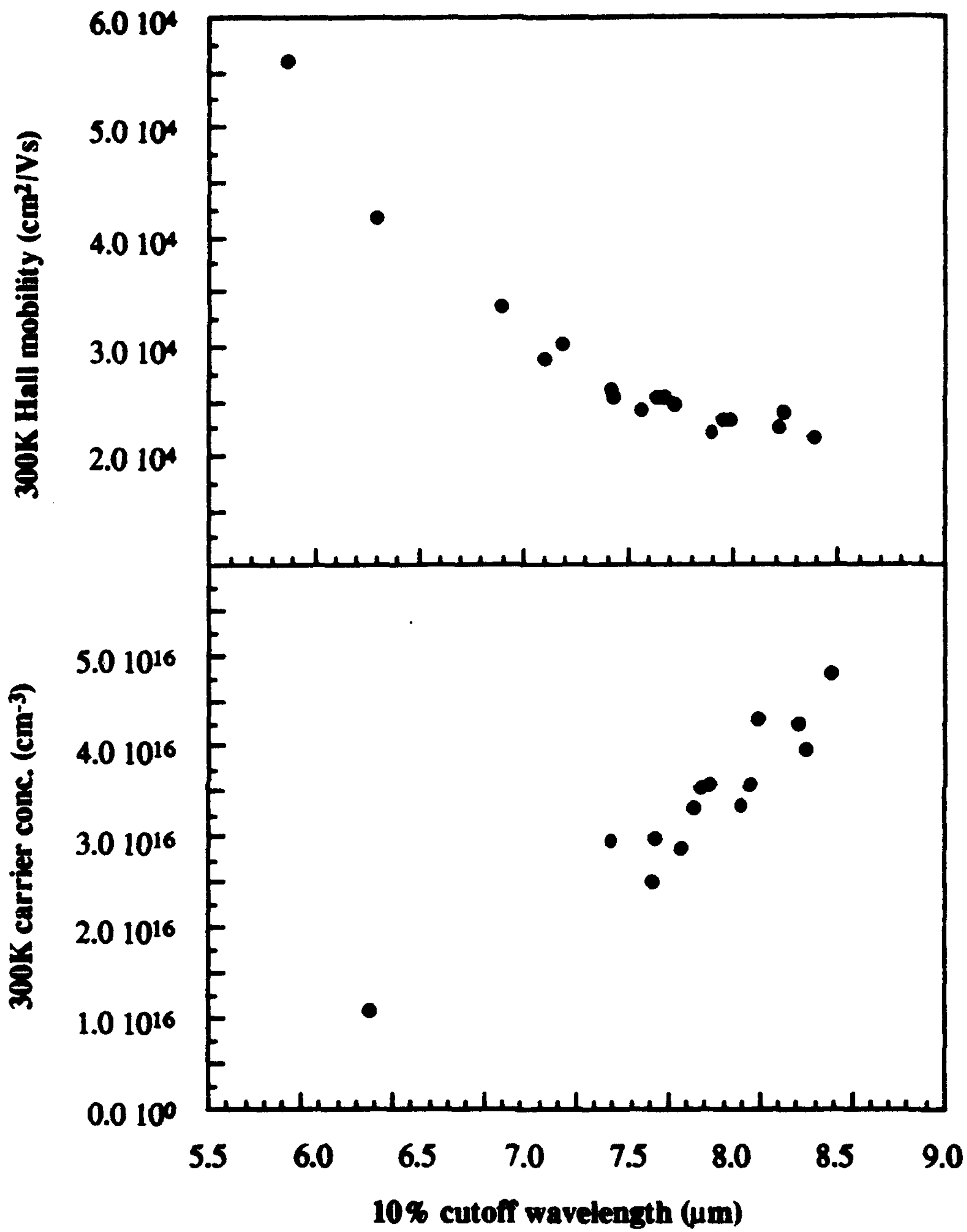

Figure 5 Room temperature Hall mobility and carrier concentration as a function of 77K photoresponse cutoff wavelength.

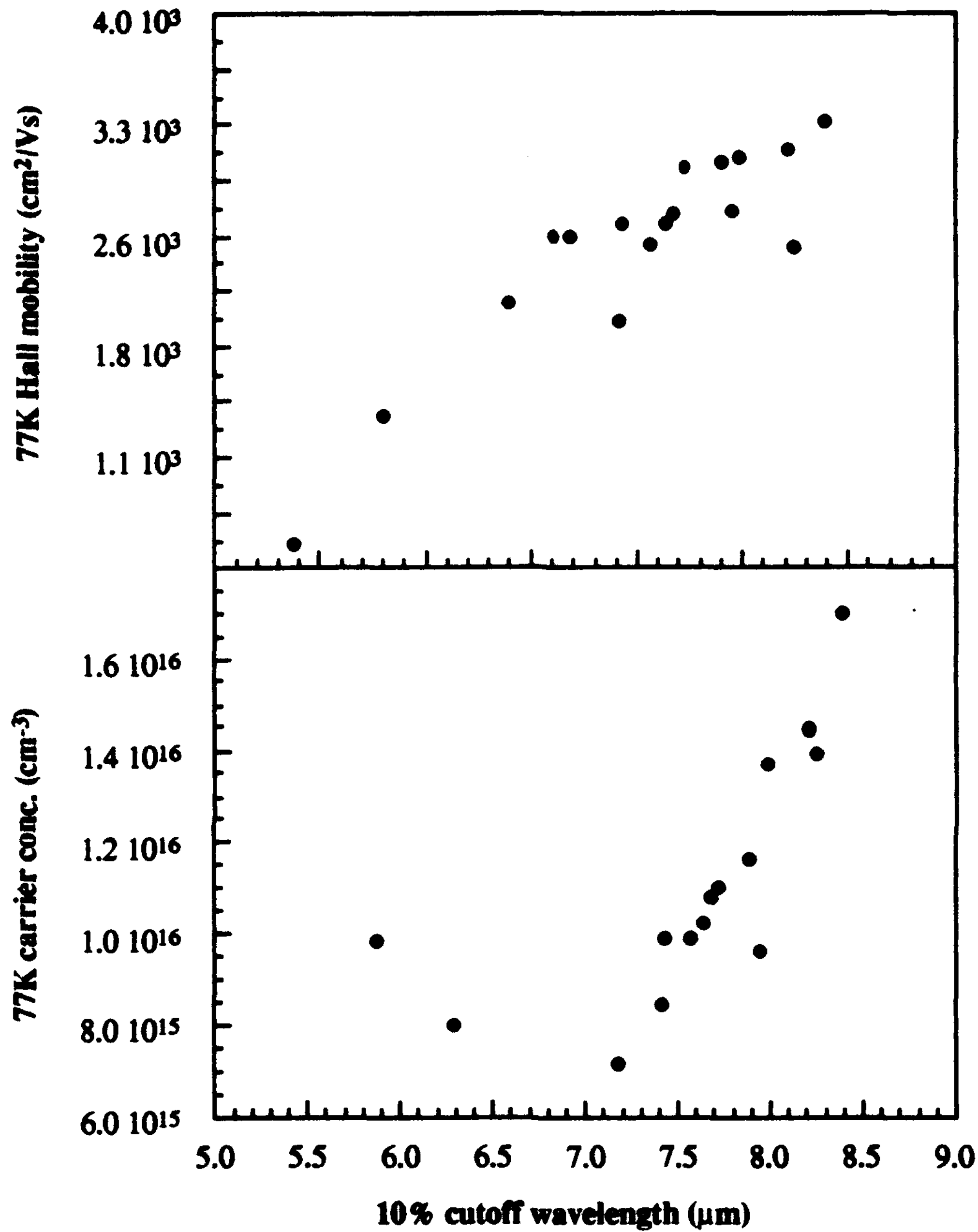

Figure 6 77K Hall mobility and carrier concentration as a function of 77K photoresponse cutoff wavelength.

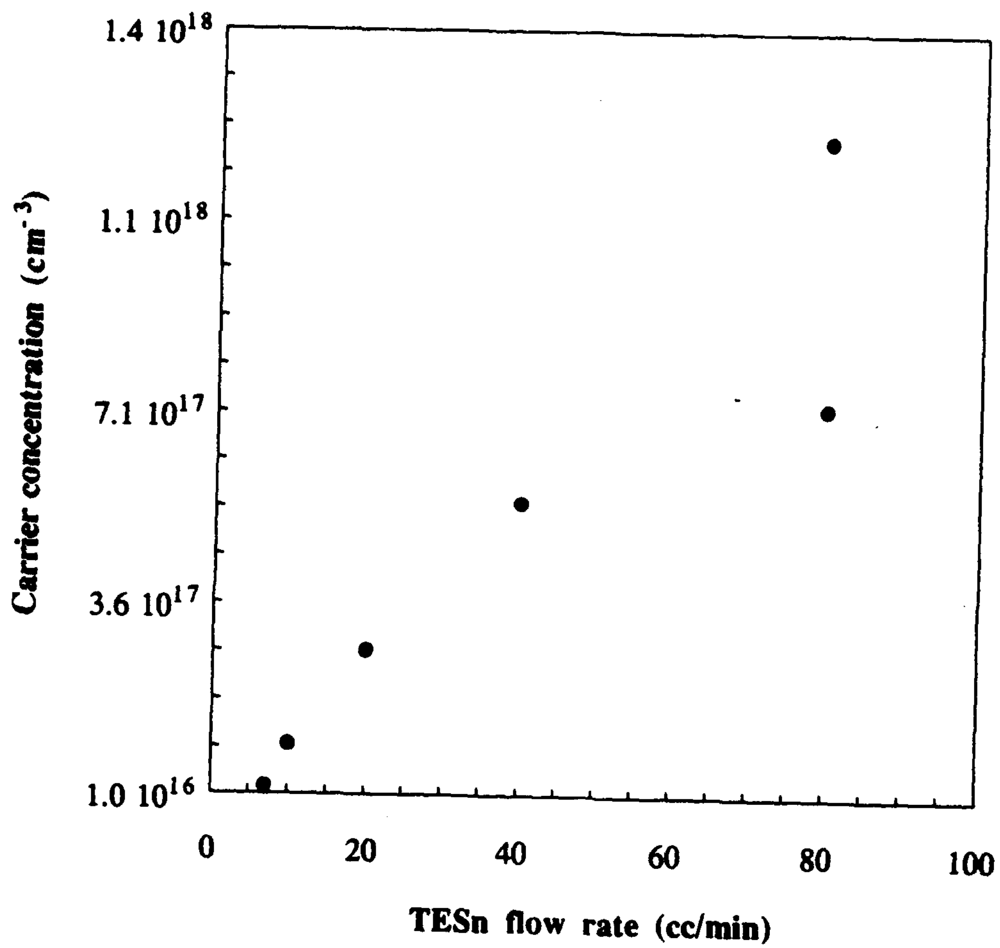

Figure 7 n-type doping concentration as a function of TESn flow rate

LIST OF PUBLICATIONS (1993-1994)

Y.H. Choi, R. Sudharsanan, C. Besikci, E. Bigan, and M. Razeghi, "High quality InSb growth on GaAs and Si by low pressure metalorganic chemical vapor deposition," *Mat. Res. Soc. Symp. Proc.* 281, 375, 1993.

C. Besikci, Y.H. Choi, R. Sudharsanan, and M. Razeghi, "Anomalous Hall effect in InSb layers grown by metalorganic chemical vapor deposition on GaAs substrates," *J. Appl. Phys.* 73, 5009, 1993.

S.N. Song, J.B. Ketterson, Y.H. Choi, R. Sudharsanan, and M. Razeghi, *Appl. Phys. Lett.* 63, 964, 1993.

Y.H. Choi, C. Besikci, R. Sudharsanan, and M. Razeghi, "Growth of $In_{1-x}Tl_xSb$, a new infrared material, by low-pressure metalorganic chemical vapor deposition," *Appl. Phys. Lett.* 63, 361, 1993.

M. Razeghi, Y.H. Choi, P.T. Staveteig, and E. Bigan, "$In_{1-x}Tl_xSb$ for long wavelength infrared detectors," *Proceedings of the 184th Meeting of the Electrochemical Society*, New Orleans, Louisiana, October, 1993.

Y.H. Choi, G. Labeyrie, P.T. Staveteig, E. Bigan, and M. Razeghi, "The effects of V/III ratio on optical, electrical, and structural properties of $InAs_{0.3}Sb_{0.7}$ grown by LP-MOCVD," *Proceedings of the 184th Meeting of the Electrochemical Society*, New Orleans, Louisiana, October, 1993.

E. Bigan and M. Razeghi, "A novel material for infrared detection: In1-xTlxSb," *Nature*, 1993.

Y.H. Choi, P.T. Staveteig, E. Bigan, and M. Razeghi, "Characterization of InTlSb/InSb grown by low-pressure metalorganic chemical vapor deposition on a GaAs substrate," *J. Appl. Phys.* 75, 1994.

P.T. Staveteig, Y.H. Choi, G. Labeyrie, E. Bigan, and M. Razeghi, "Photoconductance measurements on InTlSb/InSb/GaAs grown by low-pressure metalorganic chemical vapor deposition," *Appl. Phys. Lett.* 1994.

E. Bigan, Y.H. Choi, G. Labeyrie, and M. Razeghi, "InTlSb alloys for infrared detection," *Proceedings of SPIE*, Los Angeles, California, January, 1994.